

Charm-Anticharm Asymmetries in Photoproduction from Perturbative Recombination

Eric Braaten, Yu Jia and Thomas Mehen*

Physics Department, Ohio State University, Columbus, OH 43210, USA

(February 8, 2020)

Abstract

The asymmetries between charm and anticharm mesons observed in fixed-target photoproduction experiments are an order of magnitude larger than the asymmetries predicted by conventional perturbative QCD. We show that these charm meson asymmetries can be explained by a perturbative recombination mechanism for heavy meson production. In this process, a charm quark combines with a light antiquark from the hard-scattering process and they subsequently hadronize into a state including the charm meson. This recombination mechanism can be calculated within perturbative QCD up to some nonperturbative constants. After using symmetries of QCD to reduce the number of free parameters to two, we obtain a good fit to all the data on the asymmetries for charmed mesons from the E687 and E691 experiments.

Typeset using REVTEX

*Address after Jan. 1, 2002: Department of Physics, Duke University, Durham, NC 27708.

High energy charm photoproduction is an excellent testing ground for our understanding of strong interactions [1]. The charm quark mass provides a large scale justifying the use of perturbative QCD. Theoretical uncertainties in photoproduction are smaller than in hadroproduction because only one hadron is present in the initial state. Charm events also constitute a higher fraction of the total hadronic cross section than in hadroproduction, which facilitates experimental studies.

High energy charm photoproduction experiments [2–4] observed an interesting production asymmetry between charm and anticharm mesons. The E691 [2] and E687 [4] experiments at Fermilab measured the cross sections for various D and \bar{D} mesons from a photon beam on a beryllium target. The experiments imposed a cut on the Feynman x_F variable, $x_F > 0$, which corresponds to the forward direction of the photon beam in the γN center-of-mass frame. E691 and E687 found statistically significant asymmetries in $D^+ - D^-$, $D^0 - \bar{D}^0$ and $D^{*+} - D^{*-}$. In each case the cross section for the anticharm meson is greater, though the size of the asymmetry is different for each species of meson. Production asymmetries for D_s^+ and Λ_c^+ are also measured, but with much larger errors so they are consistent with zero. For D^+ and D^- mesons, the E687 experiment has also measured the dependence of the charm asymmetry on the photon energy, E_γ , the meson transverse momentum, p_\perp , and Feynman x_F .

The observed charm asymmetries in photoproduction are an order of magnitude larger than the asymmetries between charm and anticharm quarks predicted by perturbative QCD. Thus they cannot be understood within the fragmentation mechanism for heavy meson production which is based on the factorization theorem for inclusive single particle production [5]. In this mechanism, the c and \bar{c} are produced in a hard-scattering process and then fragment independently into charmed hadrons. At leading order in α_s , charm is produced by photon-gluon fusion [6] which produces c and \bar{c} symmetrically. The next-to-leading order (NLO) correction [7–9] increases the normalization of the total cross section by about 50% at the energies relevant to the E687 and E691 experiments. The shapes of the x_F and p_\perp distributions are similar to those at leading order, but there is a tiny charm asymmetry in these kinematic distributions, arising from the processes $\gamma + q(\bar{q}) \rightarrow c + \bar{c} + q(\bar{q})$. For $E_\gamma = 200$ GeV, the NLO calculations predict the ratio of the \bar{c} and c cross sections in the forward region to be about $R = 1.006$ [10]. The asymmetry, $(1 - R)/(1 + R) = -0.003$, is about an order of magnitude smaller than the asymmetries for D mesons measured by the E687 and E691 experiments. Furthermore, the NLO calculations cannot explain the differences in the asymmetries of D mesons with different light quark flavors. It is commonly assumed that a nonperturbative hadronization mechanism involving the remnant of the nucleon or photon after the hard scattering is responsible for the charm asymmetries.

In this paper, we argue that the charm asymmetries can be explained naturally and economically by the perturbative recombination mechanism for heavy meson production introduced in [11]. In the $\bar{c}q$ recombination mechanism, a light q from the target nucleon participates in the hard-scattering process that produces the c and \bar{c} . The light q emerges from the hard-scattering with small momentum in the \bar{c} rest frame, and the \bar{c} and q subsequently hadronize into a final state including the \bar{D} meson. There is also a $c\bar{q}$ recombination process in which a light \bar{q} from the target nucleon recombines with a c to hadronize into a D meson. Because the parton distribution functions of u and d in the nucleon are greater than the parton distribution functions for \bar{u} and \bar{d} , the recombination cross sections for $\bar{c}u$

and $\bar{c}d$ are greater than for $c\bar{u}$ and $c\bar{d}$. This gives rise to the asymmetries between charm and anticharm mesons. Since the photon participates in the hard scattering and can couple to the light quark, the recombination cross sections for processes involving u quarks differ from those involving d and s quarks because of their different electric charges. Thus, the recombination mechanism can account for the differences in the asymmetries of D mesons with different light quark flavor quantum numbers. Below we will see that the recombination mechanism can also adequately describe the kinematic dependence of the asymmetries on E_γ , p_\perp and x_F .

Before discussing the perturbative recombination mechanism in detail, we briefly review the models which have been proposed in the literature to explain the D meson asymmetries. Though these models differ in details, all generate the asymmetries by a nonperturbative hadronization process that involves the remnant of the nucleon or photon after the hard scattering. The predictions of these models depend on unknown and ad-hoc functions that specify the distribution of partons in the remnant.

The model for the asymmetry that has been most thoroughly developed involves the fragmentation of strings connecting the c and \bar{c} to the nucleon remnant [12]. After the c and \bar{c} are produced via photon-gluon fusion, the remnant of the target nucleon is left in a color-octet state. The remnant is modelled as a color-triplet “bachelor quark” and a color-antitriplet diquark with momentum fractions x and $1-x$ specified by a distribution function, $F(x)$. The subsequent hadronization is calculated using the Lund string fragmentation model [13]. Color-field strings are introduced between the diquark and the c and between the bachelor quark and the \bar{c} . The prediction for the asymmetry depends sensitively on the choice of $F(x)$ as well as the relative probability for each string to break into a charmed meson or a charmed baryon. This model reproduces the qualitative shapes of the kinematic distributions for the $D^+ - D^-$ asymmetry measured by the E687 collaboration [4]. However, the magnitude of the asymmetries is sensitive to the unknown function $F(x)$. For a “soft” distribution that diverges as $1/x$ at small x (the default option in the PYTHIA 5.6 event generator program), the model tends to overestimate the asymmetry in all kinematic regions. However, the data can be fit with a “hard” momentum distribution proportional to $1-x$ [4].

Models for the asymmetry that involve the remnant of the hadronic component of the photon have also been proposed. In one such model [10], a \bar{c} is produced by the hard scattering process $q\bar{q} \rightarrow c\bar{c}$ involving a \bar{q} from the photon. The \bar{c} then recombines with a q from the photon remnant to form a \bar{D} meson. The predictions depend on the distribution function for the q in the photon remnant and on a recombination function that could be calculated in principle using the Lund string fragmentation model. Another model is based on the possibility of intrinsic charm [14] in the photon. In this model [15], a \bar{q} in the resolved photon undergoes a hard scattering and the \bar{D} forms from a \bar{c} and q in the photon remnant. The prediction depends on the distribution function for the momentum fractions of the \bar{c} and q in the photon remnant and a recombination function that depends on several variables. Both of the models involve arbitrary functions that can be tuned to fit the data.

In contrast with these models, the perturbative recombination mechanism [11] generates the asymmetries within a hard-scattering process. The asymmetries are calculable in perturbative QCD up to some nonperturbative parameters related to the probability for the c and \bar{q} produced in the short-distance process to hadronize into a D meson. Because the c and \bar{q} do not necessarily have the same color, angular momentum or light quark flavor quan-

tum numbers as the final state D meson, several nonperturbative parameters appear in the calculation. However, it is possible to use heavy quark symmetry, $SU(3)$ flavor symmetry and large N_c arguments to reduce the number of parameters to two. The asymmetries can be adequately described by fitting these two parameters. Because of this, the recombination mechanism gives a very economical description of the observed asymmetries and does not rely on model-dependent assumptions about nonperturbative hadronization.

The factorization theorems of QCD [5] show that the leading contribution to the \overline{D} meson photoproduction cross section can be written as:

$$d\sigma[\gamma + N \rightarrow \overline{D} + X] = \sum_i f_{i/N} \otimes d\hat{\sigma}[\gamma + i \rightarrow c + \bar{c}] \otimes D_{\bar{c} \rightarrow \overline{D}}, \quad (1)$$

where $f_{i/N}$ is the parton distribution function for the parton i in a nucleon and $D_{\bar{c} \rightarrow \overline{D}}$ is the nonperturbative fragmentation function for \bar{c} to hadronize into \overline{D} . At leading order in α_s , the only parton that contributes is the gluon, so photon-gluon fusion dominates the cross section. At large p_\perp , Eq. (1) receives corrections suppressed by powers of Λ_{QCD}/p_\perp or m_c/p_\perp . The perturbative recombination mechanism introduced in [11] is an $O(\Lambda_{QCD} m_c/p_\perp^2)$ power correction to Eq. (1). The $\bar{c}q$ recombination contribution to \overline{D} production can be expressed as

$$d\sigma[\gamma + N \rightarrow \overline{D} + X] = f_{q/N} \otimes \sum_n d\hat{\sigma}[\gamma + q \rightarrow (\bar{c}q)^n + c] \rho[(\bar{c}q)^n \rightarrow \overline{D}]. \quad (2)$$

Making the replacement $c \leftrightarrow \bar{c}$, $q \rightarrow \bar{q}$ and $\overline{D} \rightarrow D$ in Eq. (2) gives the $c\bar{q}$ recombination contribution to D production. The notation $(\bar{c}q)^n$ in Eq. (2) indicates that the q in the final state has momentum of $O(\Lambda_{QCD})$ in the \bar{c} rest frame, and that the \bar{c} and the q are in a state with definite color and angular momentum quantum numbers specified by n . The factor $\rho[(\bar{c}q)^n \rightarrow \overline{D}]$ is a nonperturbative constant proportional to the probability for $(\bar{c}q)^n$ to evolve into a final state that includes the \overline{D} . The recombination process in Eq. (2) is an $O(\Lambda_{QCD} m_c/p_\perp^2)$ power correction to Eq. (1), because the parton cross section in Eq. (2) is suppressed by $O(m_c^2/p_\perp^2)$ relative to the parton cross section in Eq. (1) and $\rho[(\bar{c}q)^n \rightarrow \overline{D}]$ is expected to be $O(\Lambda_{QCD}/m_c)$ from heavy quark effective theory scaling arguments. Because the momentum of the light quark is $O(\Lambda_{QCD})$, the production of $(\bar{c}q)^n$ in states with $L \neq 0$ is suppressed by powers of Λ_{QCD}/p_\perp or Λ_{QCD}/m_c relative to S-waves. Therefore, it is only necessary to compute production of $(\bar{c}q)^n$ with 1S_0 or 3S_1 angular momentum quantum numbers. The $(\bar{c}q)^n$ can be in either a color-singlet or a color-octet state.

The four Feynman diagrams that contribute to the recombination process $\gamma + q \rightarrow (\bar{c}q) + c$ at lowest order in α_s are shown in Fig. 1. Since the momentum of the light quark in the final state, p'_q , is $O(\Lambda_{QCD})$ in the \bar{c} rest frame, its transverse momentum can be neglected and its light-cone momentum fraction, x_q , is $O(\Lambda_{QCD}/m_c)$. In the limit $x_q \rightarrow 0$, the diagrams in Figs. 1a), b) and d) are $O(x_q^{-1})$ while the diagram in Fig. 1c) is $O(x_q^0)$. Therefore the diagram in Fig. 1c) gives an $O(\Lambda_{QCD}/m_c)$ suppressed contribution to the recombination rate and can be neglected. The calculation is very similar to the calculation of the process $g + q \rightarrow (\bar{b}q) + b$ in [11]. Interested readers can refer to [11] for a detailed description of the calculation. Our result is identical to what is obtained if the D meson is modelled as a nonrelativistic quarkonium composed of a \bar{c} and q with $m_q \ll m_c$. In this respect, our calculations are similar to those of [16], where heavy-light meson production was calculated in

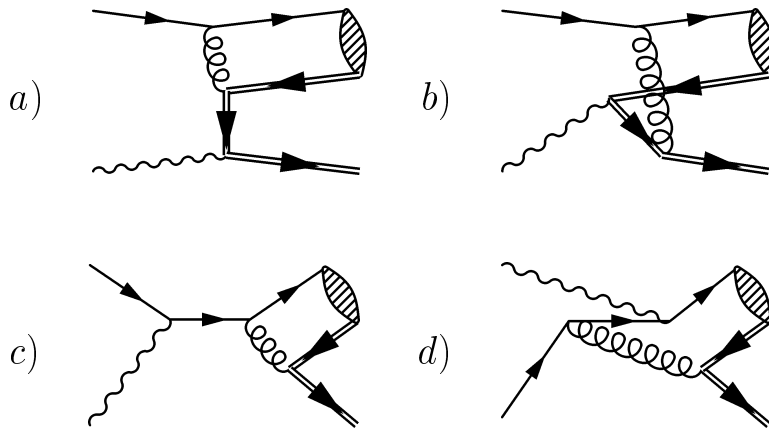


FIG. 1. Feynman diagrams for the recombination process $\gamma + q \rightarrow (\bar{c}q)^n + c$. Single lines represent a light quark and double lines represents a charm quark. The shaded blob represents $(\bar{c}q)^n$.

a quark model in which the light quark was given a small constituent mass. The color-singlet 1S_0 contribution to the cross section is obtained by first making the following substitution in the parton amplitude:

$$v_i(p_{\bar{c}})\bar{u}_j(p'_q) \longrightarrow x_q \frac{\delta_{ij}}{N_c} m_c f_+ (\not{p}_{\bar{c}} - m_c) \gamma_5. \quad (3)$$

We then set $p'_q = x_q p_{\bar{c}}$ in the rest of the amplitude and take the limit $x_q \rightarrow 0$. The nonperturbative parameter f_+ is related to the amplitude for the $(\bar{c}q)$ produced in the short-distance process to bind into a \bar{D} meson. f_+ is proportional to the D meson decay constant, f_D , times a moment of the \bar{D} meson light-cone wave function, and therefore is expected to scale as $m_c^{-1/2}$ in the heavy quark limit. However, f_+ does not account for the possibility that the $(\bar{c}q)$ can hadronize into states that include other light hadrons whose momenta are soft in the \bar{D} meson rest frame. In order to take these final states into account, f_+^2 is replaced with the parameter $\rho_1[\bar{c}q(^1S_0) \rightarrow \bar{D}]$ after squaring the matrix element. $\rho_1[\bar{c}q(^1S_0) \rightarrow \bar{D}]$ is proportional to the inclusive probability for the color-singlet, spin-singlet $(\bar{c}q)$ to evolve into any state containing the \bar{D} hadron. The calculation of the color-singlet 3S_1 cross section is identical except that γ_5 in Eq. (3) is replaced by $\not{\epsilon}$, where ϵ^μ is a polarization vector, and f_+^2 is replaced by $\rho_1[\bar{c}q(^3S_1) \rightarrow \bar{D}]$.

The \bar{D} production cross section also receives contributions from processes in which the $(\bar{c}q)$ is produced in a color-octet configuration in the short-distance process. The color-octet 1S_0 cross section is obtained by making the substitution

$$v_i(p_{\bar{c}})\bar{u}_j(p'_q) \longrightarrow x_q \sqrt{\frac{2}{N_c}} T_{ij}^a m_c f_+^8 (\not{p}_{\bar{c}} - m_c) \gamma_5 \quad (4)$$

in the parton amplitude, replacing $p'_q \rightarrow x_q p_{\bar{c}}$ and then taking the limit $x_q \rightarrow 0$. After squaring the matrix element and summing over colors in the final state, $(f_+^8)^2$ is replaced with $\rho_8[\bar{c}q(^1S_0) \rightarrow \bar{D}]$. The normalization in Eq. (4) is chosen so that ρ_8/ρ_1 is the ratio of

the probabilities for a color-octet ($\bar{c}q$) and a color-singlet ($\bar{c}q$) to hadronize into a D hadron. Finally the color-octet 3S_1 contribution is obtained by replacing γ_5 in Eq. (4) by ℓ , and replacing $(f_+^8)^2$ by $\rho_8[\bar{c}q({}^3S_1) \rightarrow \bar{D}]$.

The final results for the parton cross sections for color-singlet $\bar{c}q$ recombination in $\gamma + q$ collisions are

$$\begin{aligned} \frac{d\hat{\sigma}}{dt}[\bar{c}q({}^1S_0^{(1)})] &= \frac{256\pi^2 e_c^2 \alpha \alpha_s^2 m_c^2}{81 S^3} \left[-\frac{S}{U} \left(1 + \frac{\kappa T}{S}\right)^2 \right. \\ &\quad \left. + \frac{m_c^2 S}{U^2} \left(-\frac{S^3}{T^3} + \frac{2(1+\kappa)S}{T} + 4\kappa + \frac{\kappa^2 T}{S} \right) + \frac{2m_c^4 S^3}{T^3 U^2} \left(1 + \frac{\kappa T}{S}\right) \right], \end{aligned} \quad (5)$$

$$\begin{aligned} \frac{d\hat{\sigma}}{dt}[\bar{c}q({}^3S_1^{(1)})] &= \frac{256\pi^2 e_c^2 \alpha \alpha_s^2 m_c^2}{81 S^3} \left[-\frac{S}{U} \left(1 + \frac{2U^2}{T^2}\right) \left(1 + \frac{\kappa T}{S}\right)^2 \right. \\ &\quad \left. + \frac{m_c^2 S}{U^2} \left(\frac{S^3}{T^3} + \frac{4(2+\kappa)S^2}{T^2} + \frac{2(3+7\kappa)S}{T} + 4\kappa(3+\kappa) + \frac{3\kappa^2 T}{S} \right) \right. \\ &\quad \left. + \frac{6m_c^4 S^3}{T^3 U^2} \left(1 + \frac{\kappa T}{S}\right) \right], \end{aligned} \quad (6)$$

where $\kappa = e_q/e_c$ is the ratio of the electric charge of the light quark q to that of the charm quark, $S = (p_q + p_\gamma)^2$, $T = (p_\gamma - p_c)^2 - m_c^2$ and $U = (p_\gamma - p_{\bar{c}})^2 - m_c^2$. These variables are defined so that $S + T + U = 0$. If θ is defined as the angle between the incoming q and the outgoing ($\bar{c}q$) in the parton center-of-mass frame, then $T = -S/2[1 - (1 - 4m_c^2/S)^{1/2} \cos \theta]$. The contributions to the cross section for \bar{D} meson production are obtained by multiplying the parton cross sections in Eqs. (5) and (6) by $\rho_1[\bar{c}q({}^1S_0) \rightarrow \bar{D}]$ and $\rho_1[\bar{c}q({}^3S_1) \rightarrow \bar{D}]$, respectively. Note that the recombination process is calculated in the heavy quark limit, so we do not distinguish between m_c and the \bar{D} meson mass.

For the photoproduction diagrams in Fig. 1, the color-octet amplitude is identical to the color-singlet amplitude up to an overall color factor. The color-octet cross sections can be obtained from the color-singlet cross sections in by replacing ρ_1 with $\rho_8/8$. Therefore, recombination contributions to photoproduction cross sections depend on the following linear combination of color-singlet and color-octet parameters:

$$\rho_{\text{eff}} = \rho_1 + \frac{1}{8} \rho_8. \quad (7)$$

It is interesting to compare the relative sizes of the recombination and photon-gluon fusion cross sections in different regions of phase space. Setting $\theta = \pi/2$ and expanding in powers of m_c^2/S , one finds that the ratio of the parton cross sections is

$$\frac{d\hat{\sigma}[\gamma + q \rightarrow (\bar{c}q) + c]}{d\hat{\sigma}[\gamma + g \rightarrow \bar{c} + c]} \bigg|_{\theta=\pi/2} \approx \frac{64\pi(2-\kappa)^2}{81} \alpha_s \frac{m_c^2}{S} \quad \text{for } \bar{c}q({}^1S_0), \quad (8)$$

$$\approx \frac{64\pi(2-\kappa)^2}{27} \alpha_s \frac{m_c^2}{S} \quad \text{for } \bar{c}q({}^3S_1). \quad (9)$$

For $\theta = \pi/2$, $S = 4(p_\perp^2 + m_c^2)$, so the parton cross section for recombination is suppressed by m_c^2/p_\perp^2 at large p_\perp . The recombination cross sections are therefore suppressed by $\Lambda_{QCD} m_c/p_\perp^2$ relative to the photon-gluon fusion cross section, in accord with the factorization theorem.

The differential cross section is finite as $\theta \rightarrow 0$ and $\theta \rightarrow \pi$ because the heavy quark mass acts as an infrared cutoff. Setting $\theta = 0$ and expanding in m_c^2/S , one finds that the ratio of the two parton cross sections is

$$\frac{d\hat{\sigma}[\gamma + q \rightarrow (\bar{c}q) + c]}{d\hat{\sigma}[\gamma + g \rightarrow \bar{c} + c]} \bigg|_{\theta=0} \approx \frac{256\pi}{81}\alpha_s \quad \text{for } \bar{c}q(^1S_0), \bar{c}q(^3S_1). \quad (10)$$

Thus, the recombination cross sections have no kinematic suppression factor when the $(\bar{c}q)$ emerges from the parton collision in the same direction as the incident q . On the other hand, the recombination cross sections are suppressed by factors of m_c^2/S when the $(\bar{c}q)$ emerges in the same direction as the incident photon:

$$\frac{d\hat{\sigma}[\gamma + q \rightarrow (\bar{c}q) + c]}{d\hat{\sigma}[\gamma + g \rightarrow \bar{c} + c]} \bigg|_{\theta=\pi} \approx \frac{256\pi}{81}\alpha_s \frac{m_c^6}{S^3} \quad \text{for } \bar{c}q(^1S_0), \quad (11)$$

$$\approx \frac{512\pi(1+\kappa^2)}{81}\alpha_s \frac{m_c^2}{S} \quad \text{for } \bar{c}q(^3S_1). \quad (12)$$

The kinematic suppression is especially strong in the 1S_0 case.

To analyze the photoproduction data of E687 and E691, it is necessary to compute the cross section for various species of D mesons. It is important to realize that the color, angular momentum and light quark flavor quantum numbers of the $(c\bar{q})^n$ are not necessarily the same as the D meson in the final state [11]. The transition from the $(c\bar{q})^n$ to the final state that includes the D meson is governed by nonperturbative physics that can change these quantum numbers. For instance it is possible for the $(c\bar{q})$ to be produced in a color-octet state in the short-distance process and emit soft gluons during the nonperturbative transition to emerge as a color-singlet D meson. It is also possible for the spin of the light quark to be flipped during this transition, resulting in a D meson with different angular momentum. Finally, a light $q'\bar{q}'$ pair can be created in the transition, followed by the c binding with the \bar{q}' to form a D meson with different flavor quantum numbers than the original $(c\bar{q})^n$. Thus for a specific D meson, several nonperturbative parameters enter the calculation. For instance, for the D^0 meson, the parameters are $\rho_{\text{eff}}[c\bar{u}(^1S_0) \rightarrow D^0]$ and $\rho_{\text{eff}}[c\bar{u}(^3S_1) \rightarrow D^0]$, together with those obtained by replacing \bar{u} with \bar{d} or \bar{s} .

Symmetries of the strong interaction allow us to greatly reduce the number of free parameters. Heavy quark spin symmetry [17] implies that the spin of the c quark should remain unchanged throughout the nonperturbative transition. This means that transitions which can be related by flipping the spin of the heavy quark in both the initial and final state should have the same rate. For example,

$$\rho_{\text{eff}}[c\bar{d}(^1S_0) \rightarrow D^0] = \rho_{\text{eff}}[c\bar{d}(^3S_1) \rightarrow D^{*0}]. \quad (13)$$

One can also use $SU(3)$ light quark flavor symmetry to relate nonperturbative transitions with different light quark flavors. An example of an $SU(3)$ relation is

$$\rho_{\text{eff}}[c\bar{u}(^1S_0) \rightarrow D^0] = \rho_{\text{eff}}[c\bar{d}(^1S_0) \rightarrow D^+] = \rho_{\text{eff}}[c\bar{s}(^1S_0) \rightarrow D_s^+]. \quad (14)$$

Finally, one can argue that in the large N_c limit of QCD, light quark-antiquark pair production is suppressed. This suppression in low energy QCD is the basis for the phenomenologically successful Zweig's rule. Suppression of light quark-antiquark pair production in the

long-distance transition then forces the $(c\bar{q})^n$ to have the same flavor quantum numbers as the final state D meson.

Using the symmetries discussed above as well as large N_c arguments, one is left with two parameters. One is

$$\begin{aligned}\rho_{\text{sm}} &= \rho_{\text{eff}}[c\bar{u}(^1S_0) \rightarrow D^0] = \rho_{\text{eff}}[c\bar{d}(^1S_0) \rightarrow D^+] = \rho_{\text{eff}}[c\bar{s}(^1S_0) \rightarrow D_s^+] \\ &= \rho_{\text{eff}}[c\bar{u}(^3S_1) \rightarrow D^{*0}] = \rho_{\text{eff}}[c\bar{d}(^3S_1) \rightarrow D^{*+}] = \rho_{\text{eff}}[c\bar{s}(^3S_1) \rightarrow D_s^{*+}].\end{aligned}\quad (15)$$

The subscript sm stands for spin-matched, since in all these transitions, the spin of the $c\bar{q}$ is the same as the spin of the D meson. The other parameter describes transitions in which the light quark has its spin flipped:

$$\begin{aligned}\rho_{\text{sf}} &= \rho_{\text{eff}}[c\bar{u}(^3S_1) \rightarrow D^0] = \rho_{\text{eff}}[c\bar{d}(^3S_1) \rightarrow D^+] = \rho_{\text{eff}}[c\bar{s}(^3S_1) \rightarrow D_s^+] \\ &= \rho_{\text{eff}}[c\bar{u}(^1S_0) \rightarrow D^{*0}] = \rho_{\text{eff}}[c\bar{d}(^1S_0) \rightarrow D^{*+}] = \rho_{\text{eff}}[c\bar{s}(^1S_0) \rightarrow D_s^{*+}].\end{aligned}\quad (16)$$

While the use of heavy quark and $SU(3)$ symmetry greatly reduces the number of parameters, it should be kept in mind that these relations are only expected to hold at the 30% level. It is also important to note that the flavor-changing transitions are not strongly suppressed because $N_c = 3$. The relevant nonperturbative parameters for these transitions are expected to be smaller than ρ_{sm} and ρ_{sf} but nonvanishing. These are not included in the calculations of this paper because an adequate fit to E687 and E691 data can be obtained using only the two parameters ρ_{sm} and ρ_{sf} . However, it may be necessary to include flavor-changing transitions in other applications, or if the accuracy of current data on charm asymmetries significantly improves.

It is important to note that when a \bar{D} is produced by a $\bar{c}q$ recombination process, the associated c quark can produce a D meson via the usual fragmentation mechanism. Therefore, the recombination process can contribute to the direct cross section for D mesons in two ways:

$$a) \quad \sum_n d\hat{\sigma}[\gamma + \bar{q} \rightarrow (c\bar{q})^n + \bar{c}] \rho_n[(c\bar{q})^n \rightarrow D], \quad (17)$$

$$b) \quad \sum_{q,n} d\hat{\sigma}[\gamma + q \rightarrow (\bar{c}q)^n + c] \rho_n \otimes D_{c \rightarrow D}. \quad (18)$$

In *a*), the $(c\bar{q})^n$ recombines into the D meson. In *b*), the $(\bar{c}q)^n$ recombines into a \bar{D} meson, and the D comes from the fragmentation of the recoiling c . For direct \bar{D} production, Eq. (17) and Eq. (18) are replaced with their charge conjugates. Process *a*) produces more D^- and \bar{D}^0 mesons than D^+ and D^0 , simply because the nucleon contains more u and d than \bar{u} and \bar{d} . In process *b*), D 's are produced when there is a q in the initial state, while \bar{D} 's are produced when there is a \bar{q} in the initial state. The excess of u and d over \bar{u} and \bar{d} in the nucleon then leads to more D than \bar{D} . It turns out that in the case of $D^+ - D^-$ and $D^0 - \bar{D}^0$ mesons, process *b*) dilutes the asymmetry produced in *a*). For D_s mesons, process *a*) cannot generate an asymmetry because the s and the \bar{s} content of the nucleon are identical. Process *b*) generates an asymmetry for $D_s^+ - D_s^-$ which has the opposite sign as the $D^+ - D^-$ and $D^0 - \bar{D}^0$ asymmetries.

Finally, when computing the inclusive cross section for D and D^* mesons, one must consider the possibility of feeddown from other D mesons that are produced via photon-gluon fusion or recombination and then decay to D or D^* . The feeddown from excited

D mesons, e.g. D_2^* , is not included but is expected to be small. Therefore, the inclusive D^* cross section is the sum of the photon-gluon fusion and recombination contributions, which will be referred to as the direct cross section. The inclusive D meson cross section also includes feeddown from D^* mesons. Denoting the direct cross sections by σ_{dir} and the inclusive cross sections by σ_{inc} , one finds

$$\sigma_{\text{inc}}[D^+] = \sigma_{\text{dir}}[D^+] + 0.323 \sigma_{\text{dir}}[D^{*+}] , \quad (19)$$

$$\sigma_{\text{inc}}[D^0] = \sigma_{\text{dir}}[D^0] + 0.677 \sigma_{\text{dir}}[D^{*+}] + \sigma_{\text{dir}}[D^{*0}] , \quad (20)$$

$$\sigma_{\text{inc}}[D_s^+] = \sigma_{\text{dir}}[D_s^+] + \sigma_{\text{dir}}[D_s^{*+}] . \quad (21)$$

The coefficients of $\sigma_{\text{dir}}[D^{*+}]$ in Eq. (19) and Eq. (20) are the branching fractions of D^{*+} into D^+ and D^0 [18]. The cross sections for the charge conjugate states have similar expressions.

In the calculations presented in this paper, the contribution to charm photoproduction from the hadronic component of the photon is neglected because it constitutes less than 5% of the cross section for the fixed-target experiments in the energy range $50 \text{ GeV} < E_\gamma < 400 \text{ GeV}$ [7]. The charm quark mass is taken to be 1.5 GeV and both the factorization and renormalization scales are set equal to $\sqrt{m_c^2 + p_\perp^2}$. We checked that varying this scale between $\sqrt{m_c^2 + p_\perp^2}/2$ and $2\sqrt{m_c^2 + p_\perp^2}$ has a small effect on the predicted asymmetries. The CTEQ5L [19] parton distribution functions are used. For this parton set, it is appropriate to use the one-loop running strong coupling constant with four active flavors and $\Lambda_{QCD} = 0.192 \text{ GeV}$. Since the E691 and E687 collaborations used a beryllium target, the appropriate parton distribution is a linear combination of proton and neutron parton distribution functions: $f_{i/Be} = (4/9)f_{i/p} + (5/9)f_{i/n}$.

We use the following fragmentation function for the D meson:

$$D_{c \rightarrow D}(z) = D(z; \epsilon) f_{c \rightarrow D} , \quad (22)$$

where $f_{c \rightarrow D}$ is the probability for the direct fragmentation of c into D and $D(z; \epsilon)$ is the Peterson fragmentation function [20], normalized so that $\int_0^1 D(z; \epsilon) dz = 1$. Recent OPAL measurements find $f_{c \rightarrow D^{*+}} = 0.22 \pm 0.02$ [21] and $f_{c \rightarrow D^{*0}} = 0.22 \pm 0.07$ [22]. Heavy-quark spin symmetry implies that the direct fragmentation probabilities for D^+ and D^0 are smaller by a factor of 3. The probability for fragmentation to D_s^+ is smaller by roughly a factor of 2 [1]. In this paper, the fragmentation probabilities are chosen to be

$$f_{c \rightarrow D^{*+}} = 3 f_{c \rightarrow D^+} = 0.22 , \quad (23)$$

$$f_{c \rightarrow D^{*0}} = 3 f_{c \rightarrow D^0} = 0.22 , \quad (24)$$

$$f_{c \rightarrow D_s^{*+}} = 3 f_{c \rightarrow D_s^+} = 0.11 . \quad (25)$$

These direct fragmentation probabilities add up to about 73%, and the remaining probability comes from fragmentation to charmed baryons.

Fragmentation softens the p_\perp and x_F distributions of the D mesons relative to the c quarks produced in the hard scattering process. The measured values of the Peterson parameter ϵ range from 0.04 to 0.13 [18] depending on the D hadron. It is worth noting that the measured values of ϵ for D mesons tend to be larger than for D^* mesons. Larger ϵ corresponds to a softer D meson distribution. The softening of the D meson fragmentation function is due primarily to the feeddown contributions from D^* decay. For simplicity,

we neglect the softening of the D meson fragmentation function and use a common value $\epsilon = 0.06$ for all D and D^* mesons. Varying ϵ between 0.04 and 0.13 has a minimal effect on the predictions for the asymmetries.

Measurements of the charge asymmetry for a specific D meson are usually expressed either in terms of the anticharm/charm production ratio defined by

$$R[D] = \frac{\sigma_{\text{inc}}[\bar{D}]}{\sigma_{\text{inc}}[D]}, \quad (26)$$

or in terms of the asymmetry variable

$$\alpha[D] = \frac{\sigma_{\text{inc}}[D] - \sigma_{\text{inc}}[\bar{D}]}{\sigma_{\text{inc}}[D] + \sigma_{\text{inc}}[\bar{D}]} . \quad (27)$$

The E687 and E691 measurements of $R[D]$ for different species of D mesons are collected in Table I. The E687 measurements of $\alpha[D^+]$ as a function of E_γ , p_\perp^2 and x_F are shown in Figs. 2, 3 and 4, respectively. The E687 results are not corrected for the acceptance from a cut on the number of charged tracks at the photon interaction vertex, because the E687 hadronization model introduced a strong correlation between the acceptance and the asymmetries. This introduces an unknown systematic error in the comparison with theory. For both E687 and E691, we have combined the results from the 2 different decay channels of D^{*+} into single numbers. The E687 result for the 2 different decay channels for D^0 can be combined into the single number $R = 1.035 \pm 0.021$. Unfortunately, the D^0 sample from E687 was subjected to a “no D^* tag” requirement that reduced the feeddown from $D^{*+} \rightarrow D^0$ to about 20% of the total without reducing the feeddown from D^{*0} . We have attempted to undo the effects of that requirement, which only complicates the comparison with theory. A naive prediction for the fraction of D^0 ’s from D^{*+} feeddown can be obtained by neglecting recombination and using isospin and heavy-quark spin symmetry in Eq. (20): $3 \cdot 0.677 / (1 + 3 \cdot 0.677 + 3) = 34\%$. A feeddown of 20% can be obtained by reducing the fraction multiplying $\sigma[D^{*+}]$ in Eq. (20) to 0.333: $3 \cdot 0.333 / (1 + 3 \cdot 0.333 + 3) = 20\%$. The inclusive D^0 events should therefore consist of approximately $(1 + 3 \cdot 0.333 + 3) / (1 + 3 \cdot 0.677 + 3) = 83\%$ D^0 with no D^* tag events and 17% D^{*+} events. Since the observed values of α are small, the value of $\alpha[D^0]$ is simply given by the appropriately weighted values of $\alpha[D^0, \text{no } D^* \text{ tag}]$ and $\alpha[D^{*+}]$, up to corrections of order α^2 . We therefore take the E687 result for the asymmetry variable α for D^0 to be

$$\alpha[D^0] = 0.83 \alpha[D^0, \text{no } D^* \text{ tag}] + 0.17 \alpha[D^{*+}] . \quad (28)$$

We obtain $\alpha[D^0] = -0.023 \pm 0.009$, which corresponds to the value of R listed in Table I.

The E687 experiment has a broad-band photon beam with average energy $\langle E_\gamma \rangle = 200 \text{ GeV}$. To calculate the p_\perp^2 and x_F distributions, theoretical cross sections were convoluted with the photon beam spectrum of the E687 collaboration.¹ Our results are nearly identical if instead of using the real spectra, a monochromatic 200 GeV beam is used instead. For

¹A convenient parametrization of this spectrum can be found in Section 5 of [8].

the E_γ distribution, the data correspond to events collected in energy bins centered around 40, 120, 200 and 280 GeV. For simplicity, we calculated each data point with fixed photon energies corresponding to the center of each bin. Feynman x_F is defined by

$$x_F = \frac{p_z}{|p_z|_{\max}} \approx \frac{m_\perp \sinh(y)}{\sqrt{s_{\gamma N}}}, \quad (29)$$

where $m_\perp^2 = p_\perp^2 + m_c^2$, y is the rapidity of the D in the photon-nucleon center-of-mass frame and $s_{\gamma N}$ is the photon-nucleon center-of-mass energy squared. The positive z -axis is defined by the incident photon direction. We use the approximate expression for x_F in our calculations. The experimental results were all subject to the cut $x_F > 0$.

To fix the parameters ρ_{sm} and ρ_{sf} , we did a least-squares fit to the E687 data consisting of the ratios $R[D]$ for the four mesons in Table I, the p_\perp^2 distribution for $\alpha[D^+]$ consisting of the five data points in Fig. 3, and the x_F distribution for $\alpha[D^+]$ consisting of the first four data points in Fig. 4. Data from the last x_F bin was not included in the fit because the theory is expected to be less reliable near $x_F = 1$. In this corner of phase space, one expects increased uncertainty due to higher order corrections, nonperturbative fragmentation effects, the difference between the charm quark mass and D meson mass, etc. The results of a two parameter fit gives a value of ρ_{sf} that is small and negative. Since ρ_{sf} is proportional to a fragmentation probability, this negative value is unphysical. Therefore, we set $\rho_{\text{sf}} = 0$, and the fit then yielded $\rho_{\text{sm}} = 0.15$.

Theoretical predictions for the kinematic dependence of $\alpha[D^+]$ are compared to the E687 results in Figs. 2, 3 and 4. Perturbative recombination describes the observed asymmetries well. In particular, the E_γ dependence and the p_\perp^2 distribution are fit very well. The agreement with the x_F distribution is not as good, but the largest discrepancy is about 2.5σ in the last x_F bin, where theoretical errors are greatest. Predictions for the $R[D]$ ratios using the parameters $\rho_{\text{sm}} = 0.15$ and $\rho_{\text{sf}} = 0$ are compared to the E687 and E691 data in Table I. Most predictions for the $R[D]$ ratios are within 1σ of the data. However, the predictions for the $R[D^{*+}]$ ratios of both experiments are below the data by about 2.6σ . A better fit to the $R[D]$ ratios could be obtained if the larger value $\rho_{\text{sm}} = 0.3$ is chosen, but at the expense of a worse fit to the kinematic distributions for $\alpha[D^+]$.

The recombination mechanism reproduces some interesting qualitative features of the data. One feature is that the asymmetries decrease as E_γ increases. There are several effects that all tend to decrease the asymmetry. First, the ratio of quarks to gluons at small x decreases with energy. Furthermore, the ratio of q to \bar{q} at small x approaches 1, further diluting the asymmetry. Finally, the parton cross section for recombination falls faster than photon-gluon fusion as the parton center-of-mass energy grows. A second qualitative feature is that $R[D^+], R[D^{*+}] > R[D^0]$. This is largely because the recombination cross section for $\bar{c}d$ is greater than that for $\bar{c}u$. Because the beryllium nucleus is very close to an isosinglet target, the difference in these cross sections is not due to the parton distribution functions, but rather to the parton cross sections in Eq. (5) and Eq. (6). The differences appear because the coupling to the photon does not respect flavor symmetry: $\kappa = 1$ for $\bar{c}u$ and $\kappa = -\frac{1}{2}$ for $\bar{c}d$ and $\bar{c}s$.

In Fig. 5, the predicted inclusive cross sections, $d\sigma/dx_F$, for D^+ and D^- mesons are shown. Also shown is the contribution to the cross section from the leading order photon-gluon fusion process. Again we have used the E687 photon beam spectrum with $\langle E_\gamma \rangle =$

200 GeV. For $\rho_{\text{sm}} = 0.15$ and $\rho_{\text{sf}} = 0$, recombination contributes about 25% of the total cross section for both the D^+ and D^- . The cross sections are small for $x_F < 0$, however, in this region the D^- cross section is much greater than the D^+ cross section. Thus, recombination predicts that $|\alpha[D^+]|$ is largest in the region of phase space excluded by the experimental cut $x_F > 0$. This is because recombination is most important when the $(\bar{c}q)$ emerges in the forward direction of the light quark in the nucleon, as shown in Eq. (10).

The calculations of this paper neglected NLO corrections to the leading order photon-gluon fusion diagrams. If the NLO corrections are incorporated by including a K factor, the extracted value of ρ_{sm} must be multiplied by the same K factor to obtain the same asymmetry. As stated earlier, there is at least a 30% uncertainty in this parameter due to $1/m_Q$, $SU(3)$ breaking and $1/N_c$ corrections, and a similar size uncertainty in ρ_{sf} .

The perturbative recombination mechanism also can be used to calculate the asymmetries of charmed baryons such as the Λ_c^+ . Although the $\bar{c}q$ recombination mechanism will contribute at some level, the most important contribution is expected to come from cq recombination. We expect the asymmetry to be dominated by the analog of process *a*) in Eq. (17), which would lead to a positive asymmetry $\alpha[\Lambda_c^+]$. In the measurements from E687 and E691 in Table I, the central values correspond to a positive asymmetry, but the errors are large enough that the asymmetry is not statistically significant. The FOCUS experiment at Fermilab will measure the asymmetries for Λ_c^+ with much higher statistics and will also measure the asymmetries for other charmed baryons, such as Σ_c^0 , Σ_c^{++} and Σ_c^{*++} . It will be interesting to compare these measurements with the predictions of our perturbative recombination mechanism. Quantitative predictions will involve nonperturbative factors of the form $\rho[(cq)^n \rightarrow \Lambda_c^+]$. Once these are fit to reproduce the overall asymmetries, the kinematic distributions of the asymmetries will be predicted.

The perturbative recombination cross sections calculated in this paper predict that $\alpha[D_s^+]$ should have the opposite sign as $\alpha[D^+]$, $\alpha[D^0]$. However, it is important to point out that the $D_s^+ - D_s^-$ asymmetry is generated by the fragmentation of charm quarks which do not participate in direct recombination. In cq recombination, there is a process analogous to process *b*) in Eq. (18) which can dilute the asymmetry generated by $\bar{c}q$ recombination. To provide reliable predictions for $\alpha[D_s^+]$ asymmetries, both $\bar{c}q$ recombination into mesons and cq recombination into baryons need to be included.

Recent photoproduction measurements at HERA have shown that NLO calculations underestimate the D^* production rate in the forward proton direction [23]. Our perturbative recombination mechanism may be able to explain this observation. Recombination effects should be most important in the forward proton direction, because the ratio of the partonic cross sections for $\bar{c}q$ recombination and photon-gluon fusion is highest in this direction. The forward nucleon direction is excluded in fixed target photoproduction measurements by the $x_F > 0$ cut, but it is experimentally accessible at the HERA ep collider. For quantitative calculations of the charm asymmetries at HERA energies, it will be necessary to take into account the contribution of resolved photons.

A large charm asymmetry has been observed in fixed-target hadroproduction experiments, where it is called the “leading particle effect” [24]: charmed hadrons sharing a valence quark in common with the beam hadron are produced more copiously than other charmed hadrons in the forward region. Our recombination mechanism can be used to predict these asymmetries. The relevant parton processes are the same as those considered in [11] for

B meson production at the Tevatron. Because fixed-target hadroproduction involves lower energies, recombination is expected to play a more important role in these experiments. It would be interesting to see if recombination could provide a quantitative description of the leading particle effect.

We thank P. Garbincius, R. Gardner and J. Wiss for providing useful information about the E687 experiment. This work was supported by the Department of Energy under grant DE-FG02-91-ER4069 and by the National Science Foundation under Grant No. PHY-9800964.

REFERENCES

- [1] For a thorough review of heavy quark production, see S. Frixione, M. L. Mangano, P. Nason and G. Ridolfi, *Adv. Ser. Direct. High Energy Phys.* **15**, 609 (1998) [hep-ph/9702287].
- [2] J. C. Anjos *et al.* [Tagged Photon Spectrometer Collaboration], *Phys. Rev. Lett.* **62**, 513 (1989).
- [3] M. P. Alvarez *et al.* [NA14/2 Collaboration], *Z. Phys. C* **60**, 53 (1993).
- [4] P. L. Frabetti *et al.* [E687 Collaboration], *Phys. Lett. B* **370**, 222 (1996).
- [5] G. Curci, W. Furmanski and R. Petronzio, *Nucl. Phys. B* **175**, 27 (1980); J. C. Collins and G. Sterman, *ibid.* **185**, 172 (1981); J. C. Collins and D. E. Soper, *ibid.* **194**, 445 (1982).
- [6] L. M. Jones and H. W. Wyld, *Phys. Rev. D* **17**, 759 (1978).
- [7] R. K. Ellis and P. Nason, *Nucl. Phys. B* **312**, 551 (1989).
- [8] S. Frixione, M. L. Mangano, P. Nason and G. Ridolfi, *Nucl. Phys. B* **412**, 225 (1994).
- [9] J. Smith and W. L. van Neerven, *Nucl. Phys. B* **374**, 36 (1992).
- [10] E. Cuautle, G. Herrera, J. Magnin and A. Sanchez-Hernandez, hep-ph/0005023.
- [11] E. Braaten, Y. Jia and T. Mehen, hep-ph/0108201.
- [12] E. Norrbin and T. Sjostrand, *Phys. Lett. B* **442**, 407 (1998); *Eur. Phys. J. C* **17**, 137 (2000).
- [13] H.-U. Bengtsson and T. Sjostrand, *Comput. Phys. Commun.* **46**, 43 (1987).
- [14] S. J. Brodsky, P. Hoyer, C. Peterson and N. Sakai, *Phys. Lett. B* **93**, 451 (1980).
- [15] G. Herrera, A. Sanchez-Hernandez, E. Cuautle and J. Magnin, *Phys. Lett. B* **505**, 36 (2001).
- [16] A. V. Berezhnoy, V. V. Kiselev and A. K. Likhoded, *Phys. Atom. Nucl.* **63**, 1595 (2000) [*Yad. Fiz.* **63**, 1682 (2000)].
- [17] N. Isgur and M. B. Wise, *Phys. Lett. B* **232**, 113 (1989); *ibid.* **237**, 527 (1990).
- [18] D. E. Groom *et al.* [Particle Data Group Collaboration], *Eur. Phys. J. C* **15**, 1 (2000).
- [19] H. L. Lai *et al.* [CTEQ Collaboration], *Eur. Phys. J. C* **12**, 375 (2000).
- [20] C. Peterson, D. Schlatter, I. Schmitt and P. M. Zerwas, *Phys. Rev. D* **27**, 105 (1983).
- [21] K. Ackerstaff *et al.* [OPAL Collaboration], *Eur. Phys. J. C* **1**, 439 (1998).
- [22] K. Ackerstaff *et al.* [OPAL Collaboration], *Eur. Phys. J. C* **5**, 1 (1998).
- [23] S. Aid *et al.* [H1 Collaboration], *Nucl. Phys. B* **472**, 32 (1996); J. Breitweg *et al.* [ZEUS Collaboration], *Eur. Phys. J. C* **6**, 67 (1999); *Phys. Lett. B* **481**, 213 (2000).
- [24] E. M. Aitala *et al.* [E791 Collaboration], *Phys. Lett. B* **371**, 157 (1996); *ibid.* **411**, 230 (1997); G. A. Alves *et al.* [E769 Collaboration], *Phys. Rev. Lett.* **72**, 812 (1994); *ibid.* **77**, 2392 (1996); M. Adamovich *et al.* [BEATRICE Collaboration], *Nucl. Phys. B* **495**, 3 (1997); M. Adamovich *et al.* [WA82 Collaboration], *Phys. Lett. B* **305**, 402 (1993).

TABLE I. Anticharm/charm production ratio $R = N_{\bar{D}}/N_D$: experimental results from E687 and E691, and theory predictions with $\rho_{\text{sm}} = 0.15, \rho_{\text{sf}} = 0$.

Particle	E687 [4]	Theory	E691 [2]	Theory
	$\langle E_\gamma \rangle = 200 \text{ GeV}$		$\langle E_\gamma \rangle = 145 \text{ GeV}$	
D^+	1.08 ± 0.02	1.06	1.04 ± 0.03	1.07
D^0	1.047 ± 0.018	1.03	1.08 ± 0.03	1.03
D^{*+}	1.112 ± 0.024	1.05	1.190 ± 0.049	1.06
D_s^+	0.95 ± 0.10	0.91	0.92 ± 0.14	0.88
Λ_c^+	0.93 ± 0.14	-	0.79 ± 0.17	-
D^{*0}	-	1.02	-	1.02
D_s^{*+}	-	0.91	-	0.88

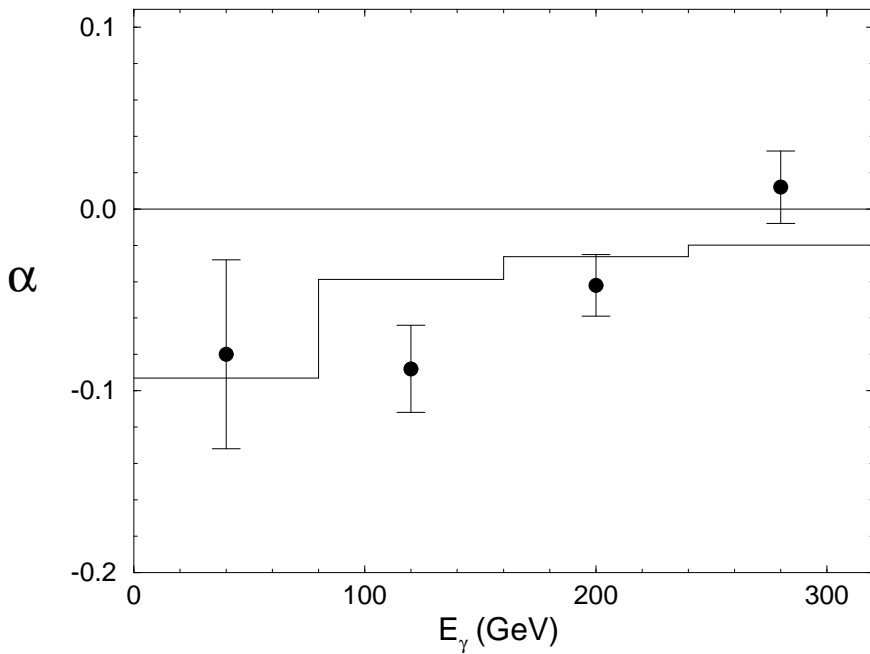


FIG. 2. The E_γ dependence of $\alpha[D^+]$. The data points are the measurements of E687 and the histogram is our prediction with $\rho_{\text{sm}} = 0.15, \rho_{\text{sf}} = 0$.

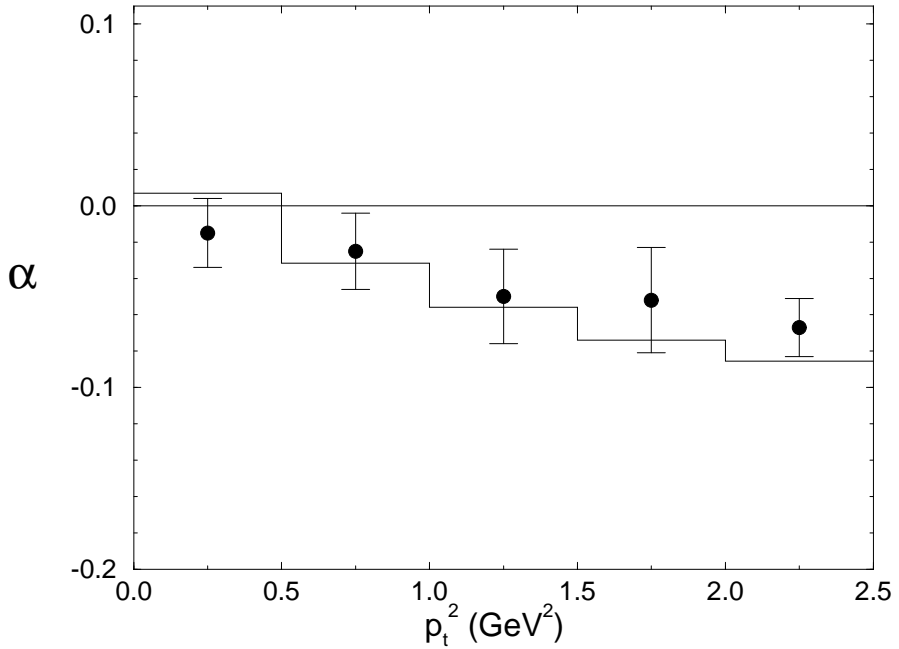


FIG. 3. The p_t^2 distribution of $\alpha[D^+]$. The data points are the measurements of E687 and the histogram is our prediction with $\rho_{\text{sm}} = 0.15$, $\rho_{\text{sf}} = 0$.

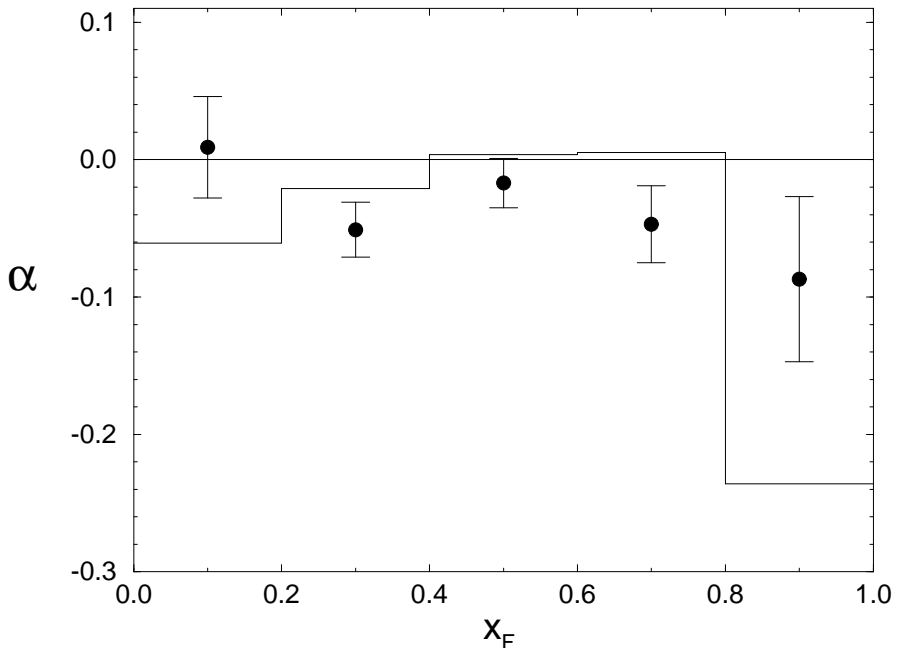


FIG. 4. The x_F distribution of $\alpha[D^+]$. The data points are the measurements of E687 and the histogram is our prediction with $\rho_{\text{sm}} = 0.15$, $\rho_{\text{sf}} = 0$.

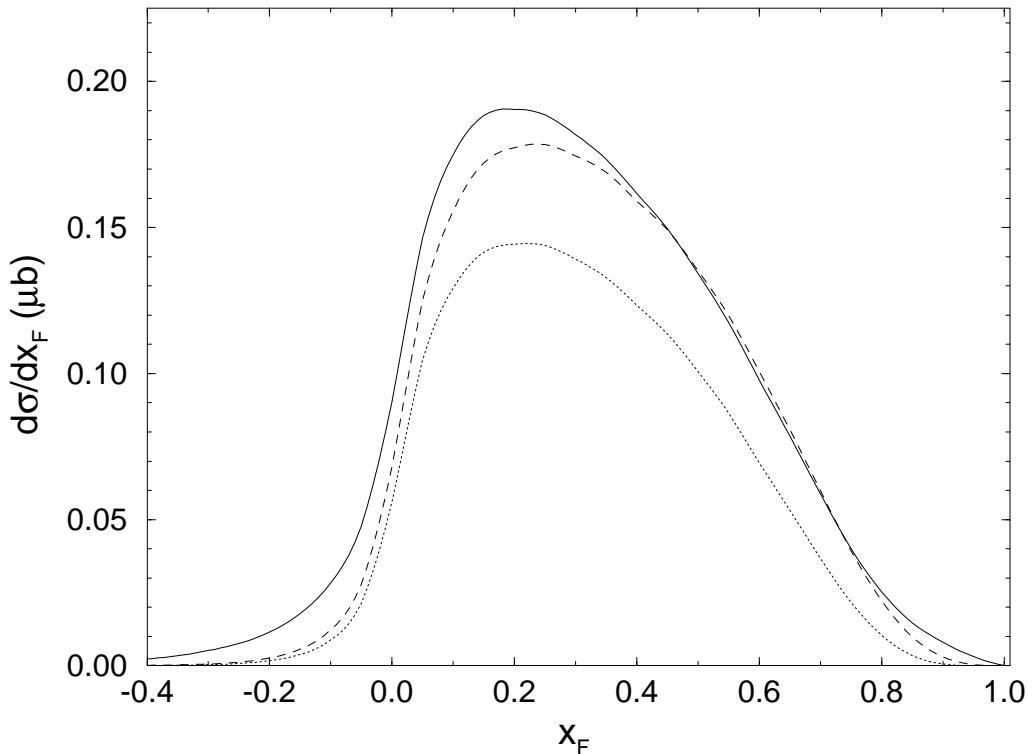


FIG. 5. Inclusive cross sections $d\sigma/dx_F$ for D^- (solid curve) and D^+ (dashed) with $\rho_{\text{sm}} = 0.15$, $\rho_{\text{sf}} = 0$. The dotted line shows the leading order photon-gluon fusion contribution to the D^\pm cross sections.